

A Bidentate Terephthalamide Ligand, TAMmeg, as an Entry into Terephthalamide-Containing Therapeutic Iron Chelating Agents[†]

Kristy M. Clarke Jurchen and Kenneth N. Raymond*

Department of Chemistry, University of California at Berkeley, California 94720-1460

Received July 29, 2005

A new bidentate 2,3-dihydroxyterephthalamide ligand, 2,3-dihydroxy-*N,N'*-bis(2-methoxyethyl)terephthalamide (TAMmeg), has been prepared. The ligand, its synthetic precursor 2,3-bis(benzyloxy)-*N,N'*-bis(2-methoxy-ethyl)-terephthalamide (BnTAMmeg), and its iron complex have been structurally characterized by X-ray diffraction. BnTAMmeg crystallizes in the monoclinic space group $P2_1/n$ with cell parameters $a = 14.4976(14)$ Å, $b = 11.5569(11)$ Å, $c = 16.3905(16)$ Å, $\beta = 113.621(1)^\circ$, and $Z = 4$. TAMmeg crystallizes in the monoclinic space group $P2_1/c$ with cell parameters $a = 13.8060(36)$ Å, $b = 8.0049(21)$ Å, $c = 19.4346(50)$ Å, $\beta = 106.855(4)^\circ$, and $Z = 4$. Fe[TAMmeg] crystallizes in the triclinic space group $P\bar{1}$ with cell parameters $a = 12.9565(14)$ Å, $b = 13.4514(14)$ Å, $c = 20.2092(21)$ Å, $\alpha = 102.093(2)^\circ$, $\beta = 95.433(2)^\circ$, $\gamma = 101.532(2)^\circ$, and $Z = 2$. The aqueous protonation and ferric ion coordination chemistry of TAMmeg were examined using potentiometric and spectrophotometric methods. Proton association constants and iron complex formation constants for the ligand are as follows: $\log \beta_{011} = 10.32$, $\log \beta_{012} = 16.49$, $\log \beta_{110} = 17.9$, $\log \beta_{120} = 32.1$, and $\log \beta_{130} = 43.0$. The ferric complex of TAMmeg is surprisingly stable for a bidentate terephthalamide iron complex. The only more-stable bidentate terephthalamide iron complex that has been reported contains a ligand with positively charged pendant arms.

Introduction

Iron is an essential nutrient whose dietary absorption and transport within the body is tightly regulated.¹ The human body has no established mechanism for iron excretion apart from blood loss. When absorption exceeds excretion, iron overload results. Iron overload is most commonly encountered either as a result of increased dietary iron absorption in the genetic disorder hemochromatosis or as a byproduct of the treatment of the genetic disorder β -thalassemia by regular blood transfusions.² This iron overload can be mediated by the administration of an organic ligand that is capable of binding iron in vivo and promoting its excretion as the iron complex. For the past 40 years, the naturally occurring siderophore desferrioxamine B (marketed under the name Desferal) has been used for this purpose; however, this therapy suffers from several drawbacks, most particularly

a cumbersome mode of administration by continuous subcutaneous infusion.³ New iron chelation therapies are needed.

This laboratory has previously reported investigations into the efficacy for iron decorporation of multidentate ligands containing the bidentate 3,2-hydroxypyridinone chelating unit.⁴ The inclusion of other bidentate iron-binding functional groups that form more thermodynamically stable iron complexes than hydroxypyridinone is anticipated to enhance the iron-chelating potential of these ligands.

The bidentate 2,3-dihydroxyterephthalamide chelating unit has been used previously in the preparation of siderophore analogues,⁵ actinide extraction agents for nuclear waste remediation,⁶ and second-generation MRI contrast agents.⁷ The strong iron-binding ability of this unit^{8,9} makes it a

[†] Paper no. 41 in the series "Ferric Iron Sequestering Agents"; for the previous paper in the series, see: Clarke Jurchen, K. M.; Raymond, K. N. *Inorg. Chem.* **2006**, *45*, 1078–1090.

* To whom correspondence should be addressed. E-mail: raymond@socrates.berkeley.edu.

(1) Andrews, N. C. *Rev. Clin. Exp. Hematol.* **2000**, *4*, 283–301.

(2) Andrews, N. C. *N. Engl. J. Med.* **1999**, *341*, 1986–1995.

(3) Hershko, C. *Rev. Clin. Exp. Hematol.* **2000**, *4*, 337–361.

(4) Yokel, R. A.; Fredenburg, A. M.; Durbin, P. W.; Xu, J.; Rayens, M. K.; Raymond, K. N. *J. Pharm. Sci.* **2000**, *89*, 545–555.

(5) Garrett, T. M.; McMurry, T. J.; Hosseini, M. W.; Reyes, Z. E.; Hahn, F. E.; Raymond, K. N. *J. Am. Chem. Soc.* **1991**, *113*, 2965–2977.

(6) Gramer, C. J.; Raymond, K. N.; Jarvienen, G. D.; Robison, T. W.; Smith, B. F. *Sep. Sci. Technol.* **2003**, *39*, 321–339.

(7) Doble, D. M. J.; Botta, M.; Wang, J.; Aime, S.; Barge, A.; Raymond, K. N. *J. Am. Chem. Soc.* **2001**, *123*, 10758–10759.

(8) Garrett, T. M.; Miller, P. W.; Raymond, K. N. *Inorg. Chem.* **1989**, *28*, 128–133.

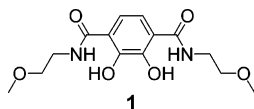


Figure 1. TAMmeg (1).

promising candidate for use in therapeutic chelators. An added advantage of terephthalamide is the ease of tailoring the properties of this unit relative to other chelating units (e.g., hydroxypyridinone) used in the development of iron chelators. Functional groups can be introduced through activation of the carboxylate groups (to the acid chloride or reactive thiazolide) at the 1 and 4 positions of the benzene ring to vary the charge, solubility, and/or biological activity of the ligand. Believing that terephthalamide-containing ligands may prove useful as potential therapeutic iron chelators, we prepared a bidentate terephthalamide with side groups compatible with biological applications (Figure 1).

To maximize bioavailability, the use of charged and/or hydrogen-bond-donating functional groups should be avoided.¹⁰ At the same time, for ease of handling in animal and clinical trials, and for thermodynamic evaluation of a ligand's chelating ability in aqueous solution, a certain degree of water solubility is desirable. To satisfy these two disparate requirements, we chose an ether-containing side chain to enhance water solubility without unduly compromising potential bioavailability. The 2-methoxyethylamide moiety should be compatible with the goal of limited ligand toxicity, on the basis of previous investigations in which a similar pyridine-based compound containing 2-methoxyethylamide units (considered for an unrelated pharmaceutical application) was found to have an acceptable toxicity profile.^{11,12}

This work details the synthesis of TAMmeg and structural and thermodynamic studies of the ligand and its iron complex. The solid-state structures of the ligand, its benzyl-protected precursor, and its iron complex were characterized by X-ray diffraction. An analysis of the solution thermodynamic behavior of this ligand reveals that it forms a surprisingly stable iron complex in comparison to other, previously evaluated bidentate terephthalamide ligands.

Results and Discussion

Synthesis. The preparation of TAMmeg (1) from commercially available catechol (2) is depicted in Scheme 1.¹³ A key intermediate in the synthesis is thiazolide-activated ester **8**. Easily prepared and purified, thiazolide intermediates are stable in alcohols, water, and dilute acids/bases and can be stored for several months without degrading. The thiazolide-activated esters react selectively with primary amines to form amide products. The completion of the reaction is indicated by the disappearance of the thiazolide intermedi-

ate's characteristic yellow color.^{14,15} The reaction produces the desired coupling product and free 2-mercaptothiazoline, which may be deprotonated and extracted from the organic product using a basic aqueous solution.

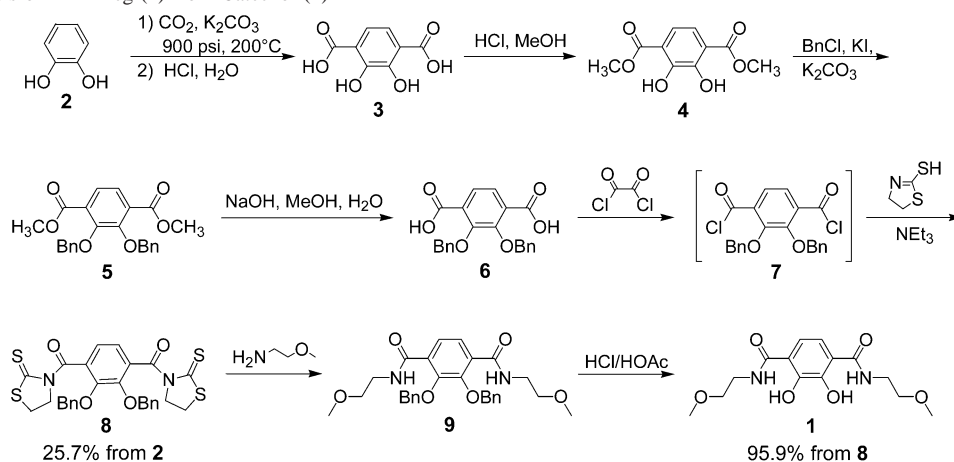
Once the thiazolide intermediate **8** has been synthesized according to literature procedures,¹³ the preparation of TAMmeg (1) is straightforward. The benzyl-protected TAM thiaz-activated ester **8** is treated with 2 equiv of 2-methoxyethylamine to afford the protected TAMmeg ligand (**9**). The free 2-mercaptothiazoline and excess 2-methoxyethylamine are then removed from the product solution with an aqueous base wash, giving the protected ligand in good yield after condensation of the solution. Cleavage of the benzyl protecting groups is accomplished under strongly acidic conditions (HCl/acetic acid), affording the deprotected ligand **1** and a small quantity of its hydrochloride salt.

The iron complex of TAMmeg was prepared by a ligand-exchange reaction with ferric acetylacetonate. A solution of 3 equiv of TAMmeg was treated with a stoichiometric amount of KOH, followed by 1 equiv of Fe(acac)₃. The metal complexation reaction proceeds very quickly, as evidenced by a rapid color change from the red-orange of ferric acetylacetonate to the deep red of the tris(terephthalamide) iron complex. To ensure complete reaction, the reaction mixture was allowed to stir for at least 1 h before the solution was condensed and the complex isolated by precipitation from ether.

Structural Characterization of BnTAMmeg, TAMmeg HCl, and Fe[TAMmeg]. Crystals suitable for diffraction were obtained of BnTAMmeg (the benzyl-protected ligand intermediate **9**), the hydrochloride salt of TAMmeg (**1**), and Fe[TAMmeg]. The high crystallinity of the compounds in this synthesis makes it possible to identify several structural features characteristic of the terephthalamide unit. BnTAMmeg crystallizes in the monoclinic space group $P2_1/n$ with $Z = 4$. As expected on the basis of previous studies,^{16,17} the amide groups are coplanar with the terephthalamide ring (Figure 2) and are held in place by hydrogen bonds between the amide protons and the phenol oxygens. The average $N_{amide}-O_{phenol}$ distance is 2.72 Å, indicating a strong hydrogen bonding interaction.¹⁸ The amide protons also hydrogen bond weakly with the ether oxygens. In this case, the average $N-O$ distance is 2.85 Å, but the amide hydrogens are not pointing directly at the ether oxygens, as the average $H-O$ distance is also 2.85 Å. Nonetheless, for both 2-methoxyethylamide side chains, the amide and ether groups adopt a sterically less-favored gauche conformation when viewed along the ethyl C-C bond, indicating that the hydrogen bond is strong enough to overcome this thermodynamic barrier. One of the benzyl aromatic rings (ring B) lies parallel to the

(9) Van Horn, J. D.; Gramer, C. J.; O'Sullivan, B.; Jurchen, K. M. C.; Doble, D. M. J.; Raymond, K. N. *C. R. Chim.* **2002**, *5*, 395–404.
 (10) Lipinski, C. A.; Lombardo, F.; Dominy, B. W.; Feeney, P. J. *Adv. Drug Delivery Rev.* **1997**, *23*, 3–25.
 (11) Horn, W. J. *Hepatology* **1991**, *13*, S63–S65.
 (12) Kellner, H. M.; Volz, M.; Badder, E.; Kurzel, G. U.; Eckert, H. G. J. *Hepatology* **1991**, *13* (Supplement 3), S48–61, discussion S62.
 (13) Doble, D. M. J.; Melchior, M.; O'Sullivan, B.; Siering, C.; Xu, J.; Pierre, V. C.; Raymond, K. N. *Inorg. Chem.* **2003**, *42*, 4930–4937.

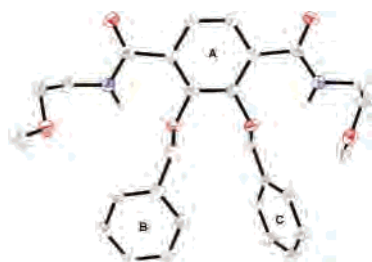
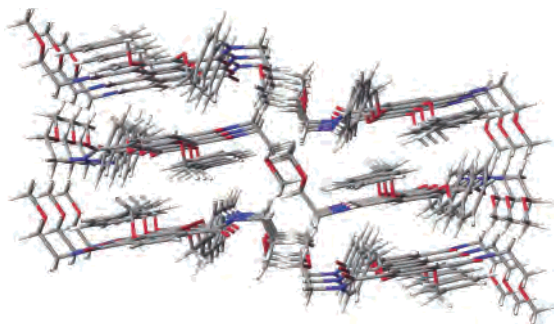
(14) Xu, J.; Kullgren, B.; Durbin, P. W.; Raymond, K. N. *J. Med. Chem.* **1995**, *38*, 2606–2614.
 (15) Nagao, Y.; Miyasaka, T.; Hagiwara, Y.; Fujita, E. *J. Chem. Soc., Perkin Trans.* **1984**, 183–187.
 (16) Karpishin, T. B.; Stack, T. D. P.; Raymond, K. N. *J. Am. Chem. Soc.* **1993**, *115*, 6115–6125.
 (17) Gramer, C. J.; Raymond, K. N. *Org. Lett.* **2001**, *3*, 2827–2830.
 (18) Jeffrey, G. A., Ed. *An Introduction to Hydrogen Bonding*; Oxford University Press: Oxford, U.K., 1997.

Scheme 1. Synthesis of TAMmeg (1) from Catechol (2)

terephthalamide ring (ring A), whereas the other (ring C) is canted $\sim 45^\circ$ relative to the plane of the other two rings. This twisting of ring C is likely a result of steric constraints caused by the proximity of ring B and of the ether side chain.

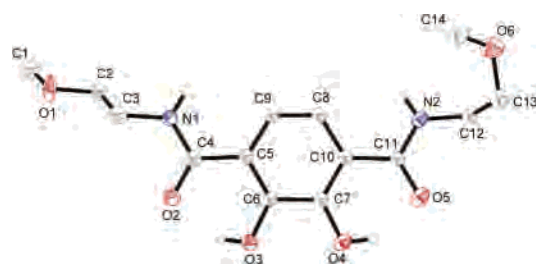
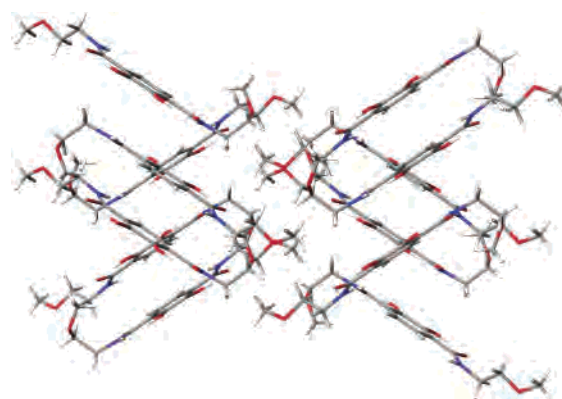
Rings A and B π -stack approximately perpendicular to the 101 vector of the crystal (Figure 3). Ring A π -stacks with both ring B and ring A on nearby molecules, whereas ring B π -stacks only with ring A. Presumably, the closest neighboring ring B is too far away (7.1 Å centroid to centroid) for the π systems to strongly interact.¹⁹ The neighboring A rings are almost perfectly lined up, as indicated by the near-equality of the distance between the ring centroids (3.799 Å) and that between the nearest C atoms (3.650 Å). On the other hand, ring A and ring B are significantly offset from each other. The centroid–centroid and nearest atom distances are very different, 4.358 and 3.456 Å, respectively.

The coplanarity of the amide groups and terephthalamide ring is also evident in the crystal structure of the deprotected

**Figure 2.** ORTEP diagram of BnTAMmeg (9) (ellipsoids at 50% level of probability).**Figure 3.** BnTAMmeg (9) π -stacking along the 101 vector.

TAMmeg ligand (Figure 4). In this case, it is the phenol protons that lock the molecule into place by hydrogen bonding with the carbonyl oxygens (average O–O distance = 2.54 Å). One of the amide protons does engage in weak hydrogen bonding with the adjacent side chain ether oxygen (N2–O6 distance = 3.05 Å), but the ether oxygen of the other side chain (O1) appears to engage only in van der Waals contact with side chains on neighboring molecules.

In the extended structure, a π -stacking network between neighboring ligands is evident (Figure 5). The centroid–centroid distance between adjacent terephthalamide rings is 3.57 Å. The crystals obtained from the deprotected ligand fell into two classes of crystal morphology, forming either large blocks or very thin (0.02 mm) plates. The large blocks gave CHN analysis consistent with the pure ligand but were too pathologically twinned to justify data collection. Collection of data with one of the thin plates gave a poor-quality

**Figure 4.** ORTEP diagram of TAMmeg (1) (ellipsoids at 50% level of probability). The atom numbering scheme is maintained in the iron complex.**Figure 5.** TAMmeg (1) π -stacking network.

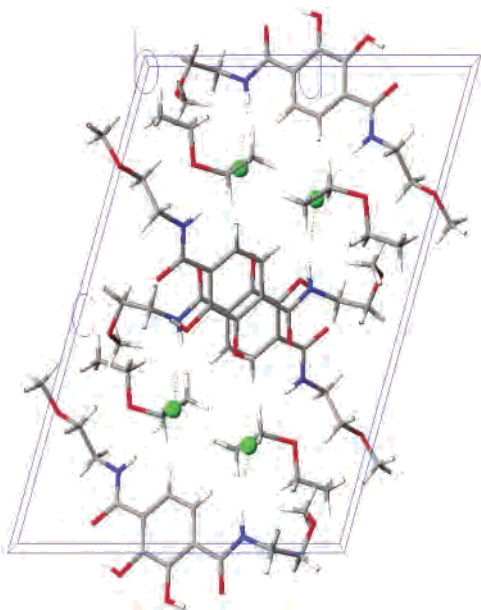


Figure 6. TAMmeg HCl unit cell.

data set with many weak reflections, and the quality of the data set made it necessary to refine all carbon atoms isotropically. Nonetheless, sufficient data were collected for accurate determination of the ligand geometry. The reason for the two distinct morphologies was discovered upon structure solution and refinement using SHELXTL.²⁰ The thin plates contain the hydrochloride salt of the ligand, the result of protonation of a small percentage of the ligand during removal of the benzyl groups under strongly acidic conditions. The chloride counterion is bound cooperatively by amide protons on two neighboring ligands (see unit cell, Figure 6). The average H–Cl distance is 2.50 Å. Because of the poor quality of the data set, the extra proton on the ligand that gives it a positive charge was not found. The proton could be either bound to one of the ether side chain oxygens or bound chelate-fashion between the phenol oxygens.

Ferric TAMmeg crystallizes as dark red plates from a DMF solution of the complex diffused with diethyl ether. The asymmetric unit contains one tris-bidentate complex, three potassium counterions, four DMF solvent molecules, and one low-occupancy water molecule. The complex displays the expected distorted octahedral geometry (Figure 7), with an average twist angle of 43.46°. The twist angle is defined as the angle between two coordinating atoms in a bidentate unit projected onto a plane perpendicular to the pseudo-3-fold axis. This twist angle is smaller than the idealized 60° twist angle for a perfect octahedron but is consistent with those of other reported metal complexes with bidentate catechol-type ligands.^{21,22} As in the protected ligand structure, the amide protons form strong hydrogen bonds with

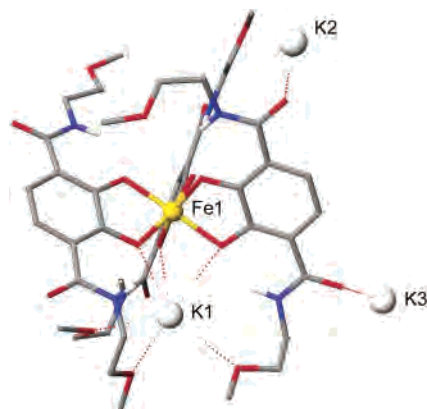


Figure 7. Ferric TAMmeg crystal structure, with potassium counterions shown.

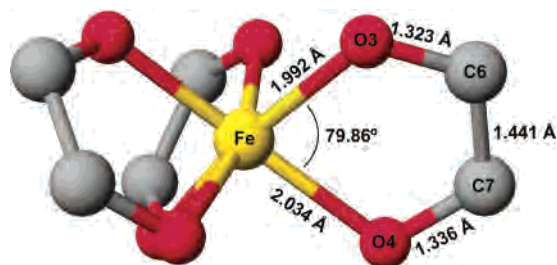


Figure 8. Chelate ring distances and angles in Fe[TAMmeg]. The values are the averages from the three chelate rings.

the phenolate oxygen atoms (average N–O distance = 2.66 Å), locking each ligand into a nearly planar geometry.

The coordination of the potassium counterions is interesting. K1 is seven-coordinate, bound by three of the phenolate oxygens (O4A–C) and the three adjacent ether oxygens (O6A–C). The seventh coordination site is occupied by a carbonyl oxygen (O5A) from a neighboring complex. The amide group on ligand A distorts out of plane to accommodate this binding carbonyl: the dihedral angle between the amide group and the aromatic ring for ligand A is 22.8°, whereas the average dihedral angle for all other amide groups in the complex is 2.3°. The other potassium counterions are not bound to phenolate oxygens. Both K2 and K3 link neighboring complexes together, bound by carbonyl oxygens from both the complexes and the DMF solvent molecules. K2 is six-coordinate, bound by three DMF oxygens and three carbonyl oxygens from neighboring complexes, and is bridged to another K2 atom by two of the DMF oxygens. K3 is only five-coordinate, bound by two DMF oxygens and three carbonyl oxygens. Two of the carbonyl oxygens link K3 to a K3 atom in a neighboring asymmetric unit.

The binding of K1 by the phenolate oxygen atoms creates an interesting asymmetry in the Fe–O bonds (Figure 8). The average of the six Fe–O bond lengths is 2.013 Å; however, the three Fe–O bonds involving the phenolate oxygens bound to K1 are on average 0.04 Å longer than the other three Fe–O bonds (2.034 vs 1.992 Å). This asymmetry would seem to suggest that the Fe–O bond is weakened by simultaneous binding of the phenolate oxygen to the iron

(19) Hunter, C. A.; Sanders, J. K. M. *J. Am. Chem. Soc.* **1990**, *112*, 5525–5534.

(20) SHELXTL, *Crystal Structure Analysis Determination Package*, version 5.10; Siemens Industrial Automation, Inc.: Madison, WI, 1997.

(21) Borgias, B. A.; Barclay, S. J.; Raymond, K. N. *J. Coord. Chem.* **1986**, *15*, 109–123.

(22) Stack, T. D. P.; Karpishin, T. B.; Raymond, K. N. *J. Am. Chem. Soc.* **1992**, *114*, 1512–1514.

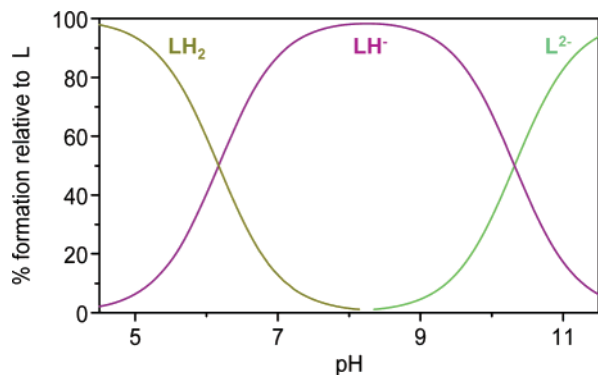


Figure 9. Speciation diagram for TAMmeg ligand.

and potassium ions. This asymmetry has not been seen in structures of tris(terephthalamide) metal complexes in which the counterion was not bound by the phenolate oxygen atoms.¹⁶

In a comparison of the three structures, some common features of the terephthalamide unit become apparent. In every case, the aromatic ring and the amide groups are coplanar. Except for the single counterexample in Fe-[TAMmeg], described above, the dihedral angles between the aromatic rings and the carbonyl groups in every structure are less than 13° and most are less than 7.5° . Hydrogen bonding plays a significant role in determining the conformation of the ligand. When the ligand is fully protonated, the preferred conformation places the carbonyl oxygen atoms closest to the phenol groups, and the resulting pattern of hydrogen bonding is outward from the phenol protons to the carbonyl oxygens. When the phenols are not protonated and thus cannot act as hydrogen bond donors, as in BrTAMmeg and Fe[TAMmeg], the oxygen atoms act as hydrogen-bond acceptors, and the preferred conformation places the amide nitrogen atoms in proximity to the phenol groups, so that the amide protons may hydrogen bond to the phenol oxygens. Hydrogen bonding also plays a role in determining the conformation of the ether side chain. In many cases, the amide protons hydrogen bond with the ether oxygens, holding the side chain in a thermodynamically less-favorable gauche conformation rather than the (all-trans) extended paraffin structure.

Solution Thermodynamics. Ligand Protonation Constants. The protonation constants for TAMmeg were determined by potentiometric titration. Each titration (forward and back) was repeated three times, with the final equilibrium constants determined by simultaneous refinement of all of the accumulated data using the Hyperquad program.²³ The bidentate ligand TAMmeg (**17**) has two dissociable protons. During the potentiometric titration experiments with this ligand, two distinct buffering regions were observed near pH 6 and 10, corresponding to the first and second proton dissociation equilibria, respectively. Refinement of the data gave final $-\log K_a$ values of 6.17(3) and 10.32(3) (Figure 9).

Metal Complexation Equilibria. Determination of the iron complex formation constant for any ligand requires the establishment of equilibrium between the metal complex and a species of known thermodynamic stability. In cases in which the metal complex can be completely dissociated by lowering the pH, making observation of the equilibrium $\text{Fe}^{3+} + \text{H}_n\text{L} \rightleftharpoons \text{FeL}^{(3-n)+} + n\text{H}^+$ possible, the ferric ion serves as the “known” variable that can be used along with the equilibrium constant determined for the reaction and the previously determined ligand protonation constants to calculate the stability constant for the iron complex, defined as K_{eq} for the equilibrium $\text{Fe}^{3+} + \text{L}^{n-} \rightleftharpoons \text{FeL}^{(3-n)+}$. Because the iron complexes of the ligands described here do not completely dissociate except at very low or negative pH values inaccessible to standard titration techniques, the iron complex formation constants were determined via competition with a ligand of known iron affinity.²⁴ EDTA is the ligand of choice for these competition experiments, as its protonation and iron complexation equilibria are well-characterized, and neither the ligand nor its iron complex absorb radiation of wavelengths greater than 420 nm.²⁵ Thus, the equilibrium $\text{FeEDTA}^- + \text{H}_n\text{L} \rightleftharpoons \text{FeL}^{(3-n)+} + \text{H}_2\text{EDTA}^{2-} + (n-2)\text{H}^+$ can be monitored at several different values of $[\text{H}^+]$ (i.e., pH) by recording the solution’s absorbance at wavelengths between 420 and 650 nm, where charge-transfer bands give TAM iron complexes their red color. Additionally, the above equilibrium is accessible in the general pH range of 2.5 to 6.0 for TAM ligands, making this equilibrium possible to monitor using standard titration techniques.²⁴

EDTA competition titrations are commonly performed in two general ways, either incrementally or in batch titrations.²⁶ In incremental titrations, a single bulk solution is used, and its pH is incrementally perturbed by the addition of a standardized acid or base solution. The solution is allowed to equilibrate for 2 h after the pH is adjusted, at which time the pH is redetermined and a UV–visible spectrum is taken. To confirm whether the solution in the incremental titrations reaches equilibrium during the 2 h delay or if the ligand-exchange reaction does not reach equilibrium during the 2 h delay period, we can also perform a batch titration. In this experiment, aliquots are removed from the bulk solution, and the pH of each aliquot is adjusted individually (concentrations are corrected for dilution). The aliquots are then allowed to reach equilibrium over a period of 48 h or more, at which time the pH of each aliquot is redetermined and a UV–visible spectrum is taken.

Once the stability of at least one representative iron complex species of the ligand in question is known, the stability of other relevant species can be determined using titrations in which only the ligand and the metal are present in solution (no EDTA), using the constant determined for the equilibrium being monitored and the formation constant for the original iron-containing species determined by EDTA

(23) Gans, P.; Sabatini, A.; Vacca, A. *HYPERQUAD2000*; Leeds, U.K., and Florence, Italy, 2000.

(24) Martell, A. E.; Motekaitis, R. J. *Determination and Use of Stability Constants*; VCH Publishers: New York, 1988.

(25) Smith, R. M.; Martell, A. E. *Critical Stability Constants*; Plenum: New York, 1977; Vol. 1–4.

(26) Cohen, S. M.; O’Sullivan, B.; Raymond, K. N. *Inorg. Chem.* **2000**, *39*, 4339–4346.

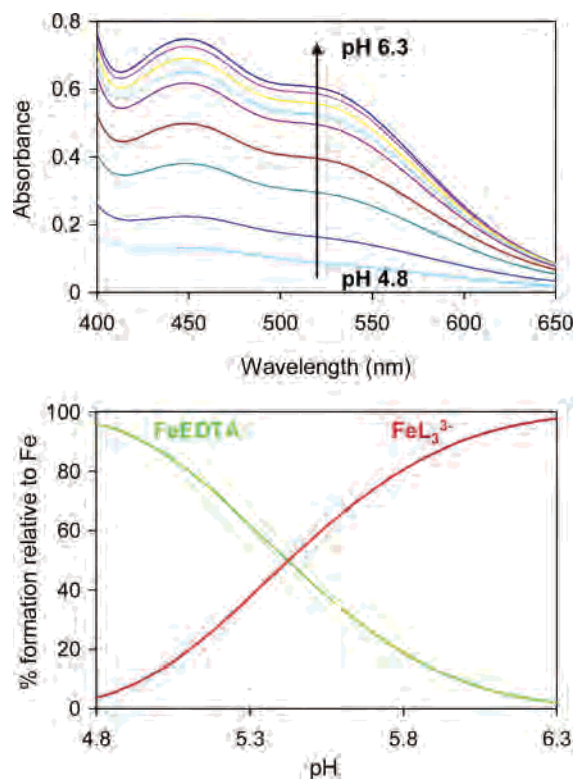


Figure 10. Sample spectra and speciation diagram for TAMmeg EDTA competition. Metal and ligand concentrations: $[\text{Fe}^{3+}] = 0.12 \text{ mM}$, $[\text{TAMmeg}] = 0.49 \text{ mM}$, $[\text{EDTA}] = 0.15 \text{ mM}$.

competition to calculate the formation constant(s) for other species that participate in the new equilibrium.²⁴

The formation constants for several iron complex species in solution must be known in order to complete the picture of TAMmeg's iron complexation behavior. As a bidentate ligand, three TAMmeg units are required to saturate iron's coordination sphere, and the formation constants β_{110} , β_{120} , and β_{130} must be determined individually. β_{130} is determined by competition titration with EDTA. A judicious selection of titration conditions permits the observation of only the $\text{FeEDTA}^- + 3\text{LH}_2 \rightleftharpoons \text{FeL}_3^{3-} + \text{H}_2\text{EDTA}^{2-} + 4\text{H}^+$ equilibrium. Three incremental titrations and one batch titration were performed over the pH range 4.8 to 6.3. At low pH (high H^+ concentration), the above equilibrium is shifted to the left and only the colorless EDTA complex is present in solution. As the pH is raised, the equilibrium shifts to the right and the charge-transfer bands typical of a tris-terephthalamide complex can be seen growing in at 450 and 510 nm (shoulder) (Figure 10). From these data, using the known ligand protonation constants and EDTA stability constants, we calculated $\log \beta_{130}$ to be 43.0(2) using the analysis program pHab.²⁷

Once β_{130} is known, β_{120} and β_{110} can both be determined in a single complex-only titration. In this titration, the sequential proton-dependent equilibria $\text{FeL}_3 + 2\text{H}^+ \rightleftharpoons \text{FeL}_2 + \text{LH}_2$ and $\text{FeL}_2 + 2\text{H}^+ \rightleftharpoons \text{FeL} + \text{LH}_2$ can be monitored. At low pH, the solution is light sea blue, the color of the monoterephthalamide complex. As the pH is raised, the color of the solution changes first to purple, the color of the bis-

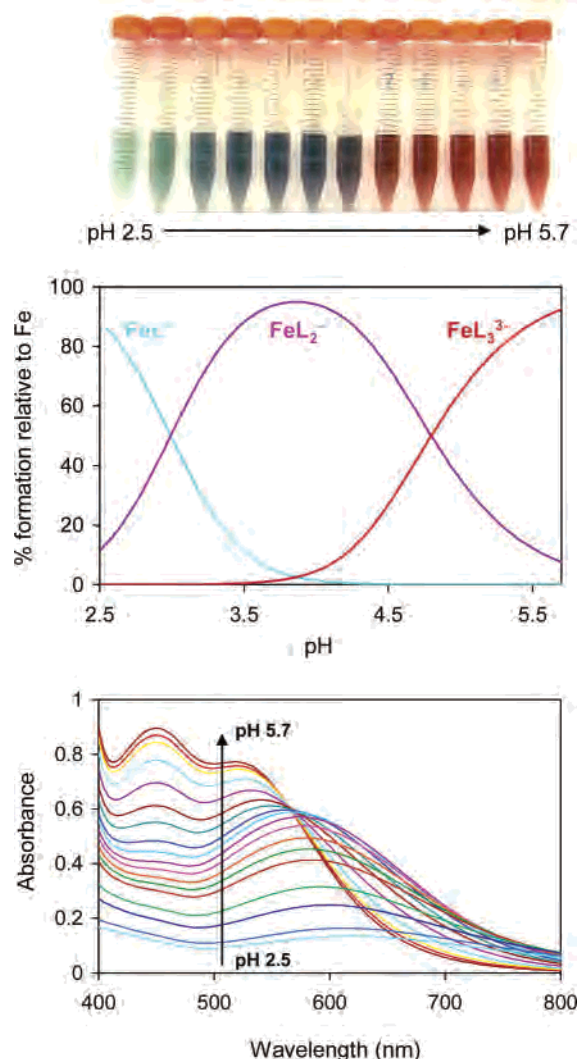


Figure 11. Color change from the FeL complex to the FeL_3 complex (top), corresponding speciation diagram (center), and UV-visual spectra (bottom). Metal and ligand concentrations: $[\text{Fe}^{3+}] = 0.16 \text{ mM}$, $[\text{TAMmeg}] = 0.49 \text{ mM}$.

terephthalamide complex, and then to red, the color of the tris-terephthalamide complex (Figure 11). Using $\log \beta_{130} = 43.0$, we determined $\log \beta_{110}$ and $\log \beta_{120}$ from the data to be 17.95(10) and 32.05(10), respectively.

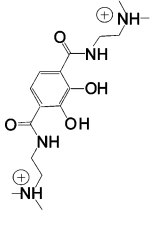
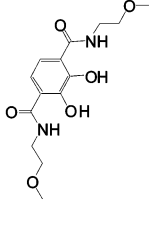
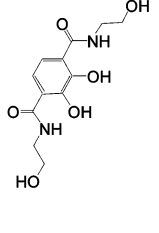
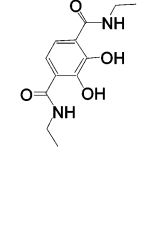
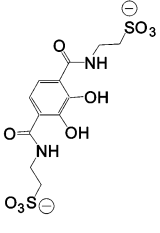
From these formation constants and the ligand protonation constants, we calculated the pM to be 24.7. The pM value for a ligand is a useful tool for evaluating the iron complex stability under physiological conditions. The pM is defined as the negative log of the free iron concentration at physiological pH (pH 7.4) with $1 \mu\text{M}$ total iron concentration and $10 \mu\text{M}$ total ligand concentration. A higher pM indicates a stronger iron complex, and pM values can be used to compare ligands of varying basicity and denticity.²⁸

It is interesting to compare the stability of the TAMmeg iron complex with the stability of the iron complexes of other, previously investigated bidentate terephthalamide ligands (Table 1). In a recent survey of various terephthalamide ligands, two with neutral side chains (DEATAM (**11**) and

(27) Gans, P.; O'Sullivan, B. *Talanta* **2000**, *51*, 33–37.

(28) Harris, W. R.; Raymond, K. N.; Weitl, F. L. *J. Am. Chem. Soc.* **1981**, *103*, 2667–2675.

Table 1. Fe(III) Chelation Constants and Ligand pKa Values for a Series of Bidentate Terephthalamides⁹ Plus TAMmeg

				
DMETAM (10)	TAMmeg (1)	DEATAM (11)	ETAM (12)	taurTAM (13)
pM = 25.4	pM = 24.7	pM = 22.9	pM = 22.8	pM = 20.4
log β ₁₁₀ = 16.9 log β ₁₂₀ = 32.7 log β ₁₃₀ = 45.3	log β ₁₁₀ = 17.9 log β ₁₂₀ = 32.1 log β ₁₃₀ = 43.0	log β ₁₁₀ = 17.0 log β ₁₂₀ = 31.0 log β ₁₃₀ = 42.1	log β ₁₁₀ = 17.3 log β ₁₂₀ = 31.6 log β ₁₃₀ = 42.7	log β ₁₁₀ = 18.2 log β ₁₂₀ = 31.7 log β ₁₃₀ = 40.3
-logKa ₁ = 5.39 -logKa ₂ = 8.43 -logKa ₃ = 9.24 -logKa ₄ = 10.86	-logKa ₁ = 6.17 -logKa ₂ = 10.32	-logKa ₁ = 6.05 -logKa ₂ = 10.61	-logKa ₁ = 6.26 -logKa ₂ = 10.83	-logKa ₁ = 6.47 -logKa ₂ = 11.01

ETAM (12)), one with positively charged side chains (DMETAM (10)), and one with negatively charged side chains (taurTAM (13)), we found that DMETAM (10) formed significantly more-stable iron complexes than the ligands with neutral or negatively charged side chains.⁹ This added stability was attributed to the ability of the *N,N*-dimethylaminoethyl side chains on the terephthalamide to offset the negative charge of the ligand–iron complex when the tertiary amines are protonated at neutral pH, thereby increasing the electrostatic attraction between partially formed complexes and additional ligands. Support for this conclusion can be found in comparing the K_2 and K_3 values for the different ligands. For DMETAM (10), the equilibrium constants for the second and third stepwise complexation equilibria are 1–2 log units greater than the same constants for the other ligands.

For TAMmeg (1), the key to its greater pM value does not lie in the second and third complexation equilibria. The K_2 and K_3 values are very close to those of ETAM and DEATAM. Instead, the major differences between TAMmeg and the other neutral-side-chain ligands lie in the first complexation equilibrium constant $\log \beta_{110}$ (at least 0.6 log units more than $\log \beta_{110}$ for ETAM (12) or DEATAM (11)) and in the first proton association constant $\log \beta_{011}$ (at least 0.3 log units less than $\log \beta_{011}$ for ETAM or DEATAM).

Conclusion

A new bidentate terephthalamide TAMmeg has been prepared as an entry into terephthalamide-containing therapeutic chelating agents. Structural studies of the protected ligand, the deprotected ligand, and the iron complex have provided evidence of hydrogen bonding between the amide

groups and the ether side chain oxygens. The ether side chains have also been shown to participate in counterion binding in the iron complex. The structural studies have also demonstrated a conformational change in the ligand upon iron binding, as both amide groups rotate by 180° between the two structures to accommodate stabilizing hydrogen bonds. This ligand forms the most-stable iron complex at physiological pH of any neutral bidentate terephthalamide ligand.

Experimental Section

Synthesis. General. Unless otherwise noted, all reagents were obtained from commercial suppliers and used without further purification. All dropwise additions were performed under a N₂ atmosphere using a pressure-equalizing addition funnel. Organic solutions were dried over anhydrous MgSO₄, and solvents were removed with a rotary evaporator. All chromatographic separations were performed using a 2 cm × 12 cm column of flash silica gel. ¹H NMR and proton-decoupled ¹³C NMR spectra were obtained in CDCl₃ solutions using a Bruker FT-NMR spectrometer operating at either 400 or 500 MHz (500 MHz unless noted otherwise), referenced to residual solvent protons. Elemental analysis and mass spectrometry were performed in the Analytical Facility in the College of Chemistry. 2,3-Dibenzoyloxy-1,4-bis(2-thioxothiazolidin-1-yl)terephthalamide (BnTAM thiaz (8)) was prepared according to procedures described in the literature.¹³

TAMmeg, Benzyl-Protected 9. BnTAM Thiaz (8) (1.20 g, 2.07 mmol) was dissolved in 30 mL of CH₂Cl₂ in a rb flask. Excess 2-methoxyethylamide (0.5 g, 6 mmol) was added via syringe, and the reaction mixture was stirred until the yellow color of the thiazolidine starting material had faded. The product solution was washed with 2 M KOH in brine (2 × 40 mL), dried, and condensed. The thick pale oil crystallized overnight to afford 9 (1.00 g, 96.5%). ¹H NMR: δ 3.24 (s, 6H, CH₃), 3.42 (t, br, 4H, CH₂), 3.54 (q, *J* =

7.2, 4H, CH₂), 5.13 (s, 4H, ArCH₂), 7.37 (m, 10H, ArH), 7.93 (s, 2H, ArH), 8.05 (t, br, 2H, NH). ¹³C NMR: δ 39.60, 58.55, 70.71, 76.73, 126.57, 128.54, 128.63, 128.70, 130.59, 135.68, 150.41, 164.25. Anal. Calcd for C₂₈H₃₂N₂O₆·0.5H₂O: C, 67.05; H, 6.63; N, 5.59. Found: C, 66.54; H, 6.68; N, 5.83.

TAMmeg (1). **9** was dissolved in a 1:1 mixture of concentrated HCl and glacial acetic acid (20 mL) and stirred overnight. The solvents were removed, and the resulting residue was coevaporated with methanol (4×). The deprotected ligand was recrystallized from acetone as small needles (0.646 g, 95.9% from **8**). ¹H NMR (DMSO-*d*₆): δ 3.25 (s, 6H, CH₃), 3.44–3.51 (m, 8H, CH₂), 7.36 (s, 2H, ArH), 8.95 (t, br, 2H, NH). ¹³C NMR (CD₃OD): δ 37.19, 46.76, 55.86, 68.64, 114.69, 116.15, 147.11, 166.89. Anal. Calcd for C₁₄H₂₀N₂O₆·0.75H₂O: C, 51.61; H, 6.65; N, 8.60. Found: C, 51.25; H, 6.73; N, 8.89. A small amount of the ligand is isolated as the hydrochloride salt; crystals of the HCl salt suitable for diffraction were obtained by slow diffusion of ether into an acetone solution of the ligand.

Metal Complexes, General Procedure. A weighed portion of the ligand was dissolved in MeOH (10 mL) and degassed by applying a slight vacuum. One equivalent of KOH (0.5 M solution in MeOH) was added to the ligand solution with a glass syringe, and the solution was degassed again. Fe(acac)₃ or Ga(acac)₃ was dissolved in MeOH (4 mL) and added to the ligand solution. The solution was degassed again and stirred for at least 1 h. The product solution was condensed to 2–4 mL and added dropwise to 20–50 mL of ether. The precipitated metal complex was isolated by centrifugation. After the supernatant was decanted, the solid was resuspended in 5 mL of ether and collected by filtration.

Fe-TAMmeg. The complex was prepared as described above using **1** (94.4 mg, 0.302 mmol), KOH (0.6 mL of a 0.5 M solution in MeOH, 0.3 mmol), and Fe(acac)₃ (35.3 mg, 0.100 mmol). Yield: 92.8 mg, 81.7%. Anal. Calcd for K₃C₄₂H₅₄N₆O₁₈Fe·2H₂O: C, 44.25; H, 5.13; N, 7.37. Found: C, 44.37; H, 5.25; N, 7.17. ESI-MS *m/z*: 1026.4 (FeL₃³⁻·K⁺·H⁺), 1010.4 (FeL₃³⁻·Na⁺·H⁺), 988.4 (FeL₃³⁻·2H⁺), 676.2 (FeL₂⁻).

Ga-TAMmeg. The complex was prepared as described above using **1** (45 mg, 0.14 mmol), KOH (0.28 mL of a 0.5 M solution in MeOH, 0.14 mmol), and Ga(acac)₃ (17 mg, 0.046 mmol). Yield: 30 mg, 53%. ¹H NMR (CD₃OD): δ 3.18 (s, 18H, CH₃), 3.35–3.45 (m, 24H, CH₂), 7.05 (s, 6H, ArH). ¹³C NMR (CD₃-OD): δ 38.28, 57.43, 70.57, 113.16, 115.79, 157.51, 169.88. Anal. Calcd for K₃C₄₂H₅₄N₆O₁₈Ga·6H₂O: C, 41.15; H, 5.43; N, 6.85. Found: C, 41.17; H, 4.94; N, 6.83.

Solution Thermodynamics, General. The titration apparatus has been described in detail by O'Sullivan et al.^{26,29,30} Corning high-performance combination glass electrodes, whose response to [H⁺] was calibrated before each titration,²⁷ were used in concert with either an Accumet pH meter or a Metrohm Titrino to measure the pH of the experimental solutions. Metrohm autoburets (Dosimat or Titrino) were used for the incremental addition of acid or base standard solutions to the titration cell. The titration instruments were fully automated and controlled using LabView software.³¹ Titrations were performed in 0.1 M KCl supporting electrolyte under positive Ar gas pressure. The temperature of the experimental solution was maintained at 25 °C by an external circulating water bath. UV–visible spectra for incremental titrations were recorded on a Hewlett-

Packard 8452a spectrophotometer (diode array). UV–visible spectra for batch titrations were recorded on a Varian Cary 300 Scan UV–visible spectrophotometer. Solid reagents were weighed on a Metrohm analytical balance accurate to 0.05 mg. Milli-Q purified water was used to prepare all solutions and was degassed prior to use by simultaneously boiling and purging with Ar. Standard solutions of 0.1 M HCl and 0.1 M KOH were prepared from JT Baker DILUT-IT ampules using freshly degassed Milli-Q purified water. The precise acid concentration was determined by titration of a sodium tetraborate solution to the methyl red endpoint. The precise base concentration was determined by titration of a potassium hydrogen phthalate solution to the phenolphthalein endpoint. Stock solutions of EDTA were obtained by dissolving disodium EDTA (Fisher) in freshly degassed Milli-Q water. The precise ligand concentration was determined by performing potentiometric titrations of the ligand solution (pH 3.5 to 8.0 and back to 3.5) in triplicate and solving for total moles of ligand using the program Hyperquad²³ by calculating the buffering capacity of the solution on the basis of published protonation constants.²⁵ Stock solutions of ferric ion were obtained by dissolving solid FeCl₃·6H₂O in standardized 0.1 M HCl. The actual ferric ion concentration was determined by titration with a standardized EDTA solution to the variamine blue endpoint.³²

Incremental Titrations. Initial titration solutions were assembled from the constituent reagents in ratios determined previously by modeling using estimated formation constants and the modeling program Hyss.^{33,34} In the case of the EDTA competition titrations, a trial titration solution was assembled and systematically varied in pH to confirm the appropriate conditions. The solutions were incrementally perturbed by the addition of either acid (HCl) or base (KOH) titrant, followed by a time delay for equilibration (90 s for protonation studies; 5–10 min for ligand–metal titrations; 2 h for EDTA competition titrations). All titrations were conducted in pairs: first, a forward titration from low to high pH, and then a reverse titration back to low pH. The data for the two titrations comprising each experiment were pooled for the calculation of formation constants. All absorbance measurements used for the calculation of formation constants were less than 1.05 absorbance units.

Batch Titrations. Bulk titration solutions were assembled from the constituent reagents as described above. Aliquots of the bulk solution were removed with a volumetric pipet and stored in plastic centrifuge tubes. The pH of each aliquot was adjusted individually using acid (HCl) or base (KOH) titrant. The aliquots were allowed to equilibrate at 25 °C for at least 48 h, at which time the final pH was determined and a UV–visible spectrum was taken of each aliquot. All absorbance measurements used for the calculation of formation constants were less than 1.05 absorbance units.

Protonation Constants. The protonation constants of TAMmeg were determined by potentiometric titration. Solutions were assembled from a weighed portion of ligand and the supporting electrolyte solution, with resulting ligand concentrations between 0.2 and 0.5 mM. A pH range from 4.5 to 11 was used. An average of 60–90 data points were collected in each pair of titrations (forward and back), each data point consisting of a volume increment and a pH reading, and the titrations were repeated three times to provide at least 180 data points for final refinement of the

(29) Johnson, A. R.; O'Sullivan, B.; Raymond, K. N. *Inorg. Chem.* **2000**, *39*, 2652–2660.

(30) Xu, J.; O'Sullivan, B.; Raymond, K. N. *Inorg. Chem.* **2002**, *41*, 6731–6742.

(31) LABVIEW, version 5.0.1; National Instruments Corp.: Austin, TX, 1998.

(32) Ueno, K.; Imamura, T.; Cheng, K. L. *Handbook of Organic Analytical Reagents*, 2nd ed.; CRC Press: Boca Raton, FL, 1992.

(33) Alderighi, L.; Gans, P.; Ienco, A.; Peters, D.; Sabatini, A.; Vacca, A. *Coord. Chem. Rev.* **1999**, *184*, 311–318.

(34) Alderighi, L.; Gans, P.; Ienco, A.; Peters, D.; Sabatini, A.; Vacca, A. *HYSS*; Leeds, U.K., and Florence, Italy, 1999.

Table 2. TAMmeg Series Crystal Data

compd	BnTAMmeg	TAMmeg·HCl	Fe[TAMmeg]
fw	492.57	422.91	1405.45
<i>T</i> (K)	121	117	129
max 2θ	49.58	49.54	50
cryst syst	monoclinic	monoclinic	triclinic
space group	$P2_1/n$	$P2_1/c$	$P\bar{1}$
<i>a</i> (Å)	14.4976(14)	13.8060(36)	12.9565(14)
α (deg)	90	90	102.093(2)
<i>b</i> (Å)	11.5569(11)	8.0049(21)	13.4514(14)
β (deg)	113.621(1)	106.855(4)	95.433(2)
<i>c</i> (Å)	16.3905(16)	19.4346(50)	20.209(2)
γ (deg)	90	90	101.532(2)
<i>V</i> (Å ³), <i>Z</i>	2516.10(51), 4	2055.56(72), 4	3340.0(6), 2
calcd density (g cm ⁻³)	1.30	1.37	1.40
cryst size (mm ³)	0.35 × 0.30 × 0.20	0.45 × 0.35 × 0.02	0.4 × 0.35 × 0.15
abs coeff μ (mm ⁻¹)	0.09	0.369	0.47
no. of reflns collected	10924	8771	16928
no. of indep. reflns	4185	3375	10729
data-to-parameter ratio	12.9	20.7	13.0
GoF on F^2	1.040	1.029	1.022
final R1 ($I > 2\sigma(I)$)	0.0444	0.1058	0.0456
final wR2	0.1123	0.2665	0.1173
R1 (all data)	0.0579	0.1787	0.0608
wR2 (all data)	0.1212	0.3194	0.1275
largest diff peak and hole (e ⁻ /Å ³)	0.18 and -0.25	0.91 and -0.87	0.56 and -0.73

ligand protonation constants. Four replicates of the potentiometric titration were performed, and refinement of the protonation constants was accomplished using the program Hyperquad,²³ which allowed simultaneous refinement of the data from multiple titration curves. The $-\log K_a$ values for TAMmeg were found to be 6.17-(3) and 10.32(3), with a global σ of 0.52 for the refinement and a correlation coefficient of 0.77 between the two protonation constants. In the course of the refinement, the molar amount of ligand used in each titration was refined; the average molecular weight calculated from these molar amounts corresponded closely with that determined by elemental analysis.

EDTA Competition Titrations. Two incremental EDTA competition titrations and a single batch titration were performed over the pH range 4.8 to 6.3 to determine the FeL₃ complex formation constant. The solutions were assembled to contain 0.12 mM Fe, 0.5 mM TAMmeg, and 0.15 mM EDTA in the supporting electrolyte. Each incremental EDTA competition experiment consisted of a pair of titrations: forward vs KOH and reverse vs HCl, with an average of 24 points collected over a period of 48 h (~2 h equilibration time per point). The batch EDTA competition experiment included nine aliquots with individually adjusted pH. At the lower-pH end of the titration, the colorless iron-EDTA complex dominated; however, as the pH was raised, the solution gradually became bright red, and the charge-transfer bands for a tris-TAM-iron complex could be seen growing in at 450 and 510 nm (broad shoulder). Each data point consisted of a pH measurement and an absorbance spectrum over at least 80 different wavelengths between 400 and 700 nm. The data were imported into the refinement program pHab³⁵ and analyzed by nonlinear least-squares refinement. During refinement of the data, factor analysis of the collected spectra indicated the presence of only one absorbing species in solution; this species was modeled as the FeL₃³⁻ complex. The previously determined TAMmeg protonation constants were included as constants, as were the literature values for the protonation and iron complex formation constants of EDTA.²⁵ Refinement of the data from the incremental and batch titrations gave very similar formation constants for the FeL₃ complex; these values were combined to give a final value for $\log \beta_{130}$ of 43.0(2).

Stepwise Formation Constant Titration. A titration was performed to determine the equilibrium constants for the stepwise proton-dependent complexation equilibria $\text{FeL}^+ + \text{H}_2\text{L} \rightleftharpoons \text{FeL}_2^- + 2\text{H}^+$ and $\text{FeL}_2^- + \text{H}_2\text{L} \rightleftharpoons \text{FeL}_3^{3-} + 2\text{H}^+$. Concentrations of 0.10–0.16 mM iron and 0.40–0.50 mM ligand were used, and the solution was titrated over the pH range of 2.5 to 5.5. At the lower pH limit, the solution is light turquoise (the monoterephthalamide complex); at intermediate pH, the solution turns purple (the bis-terephthalamide complex), and at the higher end of the pH range, the solution is bright red, the color of the tris-terephthalamide complex. Two incremental titrations and one batch titration were performed on this system. For the refinement, the previously determined ligand protonation constants and the FeL₃ formation constant were included as known constants. Refinement of the collected data gives values of $\log \beta_{110} = 17.95(20)$ and $\log \beta_{120} = 32.05(20)$ when $\log \beta_{130} = 43.0(2)$.

X-ray Crystallography. Crystals of BnTAMmeg were obtained as colorless plates by layering an oil of the pure compound with diethyl ether. Crystals of TAMmeg·HCl were obtained as very thin colorless plates from a solution in acetone diffused with diethyl ether. Crystals of potassium Fe[TAMmeg]·4DMF·0.5 H₂O were grown as dark red plates from a DMF solution diffused with diethyl ether.

Selected crystals of each compound were mounted in Paratone N oil on quartz capillaries and frozen in place under a cold N₂ stream (110–150 K, maintained throughout data collection). The crystallographic data sets were collected on a Siemens SMART X-ray diffractometer equipped with a CCD area detector using Mo K α radiation ($\lambda = 0.71072$ Å, graphite monochromator). An arbitrary hemisphere of data was collected for each crystal using ω scans of 0.3° per CCD area detector frame and a total measuring time of 10 to 35 s each (measuring time constant for each crystal). The intensity data to a maximum 2θ range of ~50° (specific 2θ different for each crystal) were integrated using SAINT with box size parameters of 1.6 × 1.6 × 0.6.³⁶ The data were corrected for Lorentz and polarization effects. An empirical absorption correction for each crystal was based on the measurement of redundant and equivalent reflections using an ellipsoid model for the absorption

(35) Gans, P.; Sabatini, A.; Vacca, A. *Ann. Chim. (Rome)* **1999**, *89*, 45–49.

(36) SAINT, SAX Area-Detector Integration Program, version 4.024; Siemens Industrial Automation, Inc.: Madison, WI, 1994.

TAMmeg as an Entry into Iron Chelating Agents

surface and was applied using SADABS.³⁷ Equivalent reflections were merged, and the space groups were determined using XPREP²⁰ on the basis of lattice symmetry and systematic absences.

The structures were solved by direct methods (SHELXS-86).³⁸ After most of the atoms had been located, the data set was refined using the SHELXTL-97 software package.²⁰ In the structure of TAMmeg HCl, the carbon atoms were refined isotropically. All other nondisordered non-hydrogen atoms were refined anisotropi-

(37) *SMART Area-Detector Software Package*; Siemens Industrial Automation, Inc.: Madison, WI, 1994.

(38) Sheldrick, G. M. *Acta Crystallogr., Sect. A* **1990**, *46*, 467–473.

cally. Unless otherwise noted, hydrogen atoms were assigned to idealized positions. Additional experimental details for each structure are summarized in Table 2.

Acknowledgment. We thank Dr. Fred Hollander and Dr. Allen Oliver for assistance with the X-ray structure determinations and Rebecca Abergel for assistance in editing. This work was supported by the National Institutes of Health (NIH Grant DK057814).

IC051287+